

# SPECT IMAGE RESTORATION VIA RECURSIVE INVERSE FILTERING CONSTRAINED BY A PROBABILISTIC MRI ATLAS

S. Benameur<sup>‡</sup>, M. Mignotte<sup>‡</sup>, J.-P. Soucy<sup>†</sup>, and J. Meunier<sup>‡</sup>

<sup>‡</sup>Image Processing Laboratory, DIRO, University of Montreal, Montreal, Canada

<sup>†</sup> Research Center of the University of Montreal Hospital Center, Montreal, Canada.

E-MAIL: BENAMEUS@IRO.UMONTREAL.CA

## ABSTRACT

3D Brain SPECT imagery is a well established functional imaging method which has become a great help to physicians in the diagnosis of several neurological and cerebrovascular diseases. However, mainly due to the effects of attenuation and the scattering of emitted photons, inherent to this imaging process, 3D SPECT images are generally blurred and exhibit poor spatial resolution. This leads to substantial errors in measurements of regional brain blood flow, and therefore in the estimations of brain activity. In order to improve the resolution of these images and then to facilitate their interpretation, we herein propose an original extension of the NAS-RIF (Recursive Inverse Filtering) deconvolution technique proposed by Kundur and Hatzinakos [1]. The proposed extension allows to efficiently integrate, in the deconvolution process, a set of *soft* constraints given by a probabilistic MRI atlas containing experts's prior knowledge about the spatial localization of the different brain structures (or tissue classes). This extension has three interesting properties; first it allows to exploit (or fuse) reliable anatomical and (high resolution) geometrical information extracted from a probabilistic 3D MRI atlas. Second, it allows to incorporate, into the NAS-RIF method, a regularization term which efficiently stabilizes the inverse solution. Third and contrary to multi-modal restoration techniques, it does not require a MRI scan of the patient. This method has been successfully tested on numerous real brain SPECT images (of different patients suffering from epilepsy), yielding promising restoration results.

**Index Terms :** *SPECT imagery, MR imagery, 3D blind deconvolution, probabilistic MRI atlas, 3D/3D registration, image restoration, information fusion.*

## 1. INTRODUCTION

The poor spatial resolution of SPECT images considerably limits the potential diagnostic of functional brain SPECT scans; for instance, it may be difficult to distinguish between low tracer uptake due to a functional deficit, where brain tissue still exists, from low uptake generated by focal atrophy, where tissue is lost and replaced by CerebroSpinal Fluid (CSF). In pathologies where both phenomena occur the interpretation of SPECT images may be problematic.

Up to now, several methods have been proposed to improve the spatial resolution of SPECT images. These methods can be split into two major classes, namely methods using restoration techniques during or after the reconstruction process from projections. In this paper, we are describing a post-tomographic reconstruction process, an

approach which has the advantage of being essentially independent from the physical features of the scanner.

In our previous work [2], we have shown that the NAS-RIF deconvolution algorithm [1] could take into account (high resolution) anatomical MRI information (from the same patient) to better constrain the deconvolution process. More precisely, the unsupervised Markovian segmentation of this (previously registered) MRI volume allowed to easily define an edge-preserving regularization term for the iterative NAS-RIF deconvolution procedure. This regularization term consisted in applying, over pre-detected and segmented anatomical regions of common tissue type, a piecewise smoothness constraint on the functional SPECT image to be restored. However, this latter restoration technique remains closely related to the accuracy of the segmented anatomical image. Besides, the very idea of boundaries (between tissue classes) is not always clear for a functional image. At the level of resolution of a SPECT image the anatomical boundaries are rarely distinct. For instance, the transition from one tissue type to another may not be highly localized and may be progressive. Consequently, the above-mentioned model is not very well suited to take into account the partial volume effect and thus can not be particularly efficient in order to permit accurate recovery of small structures.

In order to take into account the above-mentioned problems, an alternative strategy, proposed in this paper consist in considering a soft region-based anatomical constraint given by a MRI probabilistic atlas [3]. Each voxel of this atlas is associated with a  $K$ -dimensional vector which probabilistically contains the membership of this voxel to each anatomical tissue class. This *fuzzy* modeling allows each pixel to belong to several classes simultaneously (and therefore to take also into account the partial volume effect).

Probabilistic atlases are commonly used to give *a priori* information on the location and variability of the anatomy, which is then used as an initialization or to improve a segmentation procedure [4, 5, 6, 7, 8]. In another application, Chen *et al.* [10] achieved improvement in their registration method by incorporating probabilistic information on the intensity and geometric variations. To the best of our knowledge, this work remains the first to exploit a probabilistic atlas for a restoration problem. The probabilistic atlas will allow us to perform a SPECT restoration without the need of the patient's MRI scan to get the additional high resolution information and necessary constraints required for the regularisation of our ill-posed restoration problem.

This paper is organized as follows. Section 2 briefly describes the proposed 3D extended version of the NAS-RIF deconvolution technique. In Section 3, we describe the generation of the 3D MRI

atlas and Section 4 the 3D/3D registration algorithm between the MRI and SPECT data volume. In Sections 5 and 6, we show some SPECT images restoration results and conclude.

## 2. 3-D DECONVOLUTION METHOD

### 2.1. 3D extended version of the NAS-RIF

In our application, and as proposed in [11], we will assume that 3D SPECT images are degraded by the following, classical linear model

$$g(x, y, z) = f(x, y, z) * h(x, y, z) + n(x, y, z) \quad (1)$$

in which  $g(x, y, z)$ ,  $f(x, y, z)$ , and  $h(x, y, z)$ , denote respectively the degraded 3D image, the true image and the point spread function (PSF).  $n(x, y, z)$  represents the additive noise and  $*$  designates the 3D discrete linear convolution operator. The 3D blind deconvolution problem consists in determining  $f(x, y, z)$  and  $h(x, y, z)$  (or its inverse) given the blurred observation  $g(x, y, z)$ . In the 3D extended

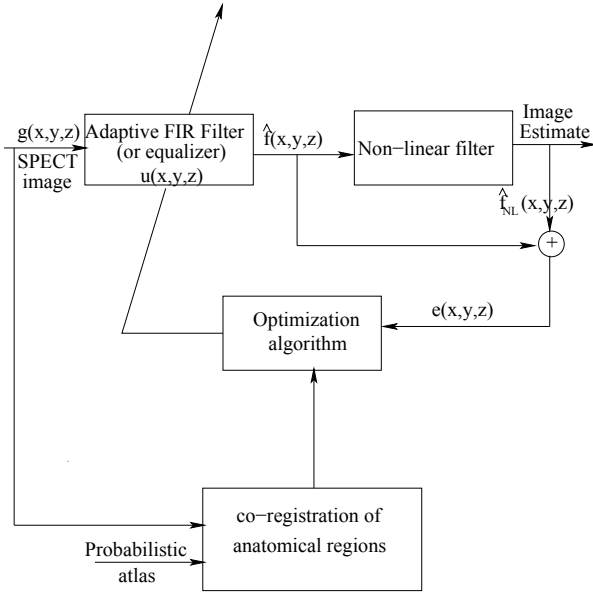


**Fig. 1.** Three-dimensional extension of the NAS-RIF deconvolution algorithm using an anatomical (MRI) atlas-based constrain.

version of the NAS-RIF deconvolution strategy (cf. Fig. 1), the output of the FIR filter  $u(x, y, z)$  of dimension  $N_{xu} \times N_{yu} \times N_{zu}$  gives an estimate of the true image  $\hat{f}(x, y, z)$ . Each resulting estimation is passed through a nonlinear filter which expresses the fact that the image is assumed to be non-negative within a known support (i.e., the organ). The difference between this projected image  $\hat{f}_{NL}$  and  $\hat{f}$  is used as the error signal to update the variable filter  $u(x, y, z)$ . In the 3D context, the cost function used in the deconvolution procedure of the 3D image is defined as :

$$J(u) = J_1(u) + J_2(u) + \gamma J_3(u) \quad (2)$$

with,

$$J_1(u) = \sum_{(x,y,z) \in \mathcal{D}} \hat{f}^2(x, y, z) \left( \frac{1 - \text{sgn}(\hat{f}(x, y, z))}{2} \right)$$

$$J_2(u) = \sum_{(x,y,z) \in \overline{\mathcal{D}}} (\hat{f}(x, y, z) - L_B)^2$$

$$J_3(u) = \left( \sum_{\forall (x,y,z)} u(x, y, z) - 1 \right)^2$$

where  $\hat{f}(x, y, z) = g(x, y, z) * u(x, y, z)$ , and  $\text{sgn}(f) = -1$  if  $f < 0$  and  $\text{sgn}(f) = 1$  if  $f \geq 0$ .  $\mathcal{D}$  is the set of all pixels of  $g(x, y, z)$  inside the region of support (i.e., inside the brain), and  $\overline{\mathcal{D}}$  is the set of all pixels outside the region of support.

The first term,  $J_1(u)$ , is used to penalize the negative voxels in the support in order to keep the image estimate non-negative. The second term  $J_2(u)$  penalizes voxels located outside the support which show values which deviate significantly from the background average  $L_B$ . When the background of the true image is black, i.e.,  $L_B = 0$ , the third term,  $J_3(u)$ , is used to avoid a trivial all-zero minimum solution ( $\gamma$  being a positive constant).

### 2.2. Atlas-Based Anatomical Constraint 3D NAS-RIF

The major shortcoming of the NAS-RIF technique is its noise amplification at low SNR [12]. This is due to the high pass property of the inverse filter  $u(x, y, z)$  which amplifies high frequency noise. As a result, the solution at convergence may not be the best estimate of the original image in the presence of noise. In order to solve this problem, a solution, suggested by Kundur and Hatzinakos [12], consists in halting the iterative restoration process through visual inspection. In practice, this requires a strong supervision and, even in this case, it is not so easy to determine which is the optimal iteration for termination (different parts of the image may converge at different rates, making this method unreliable).

In this work, we propose an alternative regularization approach for the NAS-RIF algorithm which can also be viewed as an elegant way to fuse geometrical information extracted from a probabilistic 3D MRI atlas with the SPECT data to be restored. The proposed regularization term also allows stabilization of the inverse solution of the NAS-RIF procedure (by preventing noise amplification), does not require supervision (parameter tuning or stopping criterion) and is capable of introducing better constraints on the solution of our restoration problem. This strategy consists in applying, a set of *soft* constraints given by a probabilistic MRI atlas (previously registered with the SPECT image) containing prior knowledge about the spatial localization of the different tissue classes. More precisely, this MRI atlas-based constraint is taken into account via a new additional regularization term  $J_4(u)$  which consists in applying, a *soft* piecewise smoothness constraint, probabilistically weighted according to the membership of each voxel to each anatomical tissue class.

In our model, the new cost function related to the deconvolution of the 3D image can be written as

$$J(u) = J_1(u) + J_2(u) + \gamma J_3(u) + \delta J_4(u) \quad (3)$$

with :

$$J_4(u) = \sum_{i=1}^3 \sum_{(x,y,z) \in r_i} P_i(x, y, z) (\hat{f}(x, y, z) - \bar{r}_i)^2 \quad (4)$$

The first summation is made on the three main anatomical tissue regions ( $r_i$ ) found in the brain, i.e., white matter ( $r_1$ ), grey matter ( $r_2$ ), and cerebro-spinal fluid ( $r_3$ ).  $P_{r_i}(x, y, z)$  is the probability given by the registered MRI atlas for a voxel at location  $(x, y, z)$  to

belong to the anatomical tissue class  $r_i$ ,  $\bar{r}_i$  designates the mean, in grey level, of the  $i^{\text{th}}$  region and  $\delta$  is a weighting factor between this *soft* anatomical constraint and the remaining hard constraints of the NAS-RIF procedure. In this context,  $\mathcal{D}$  designates the brain support ( $\mathcal{D} = r_1 \cup r_2 \cup r_3$ ) and  $\bar{r}_i$  ( $i \in \{1, 2, 3\}$ ) is updated at each iteration of the NAS-RIF deconvolution procedure by the expectation of the empirical mean estimator

$$\bar{r}_i = \frac{1}{N_i} \sum_{(x,y,z) \in r_i} P_i(x,y,z) \hat{f}(x,y,z) \quad (5)$$

where  $N_i$  is the cardinal of the region  $r_i$ .

$J_4(u)$  is thus proportional to the sum of variances of each anatomical region (using the *fuzzy* empirical mean and variance estimators) of the SPECT image. This term expresses that, according to our belief in the belonging of each tissue class (given by  $P_{r_i}(x,y,z)$ ), voxels in the functional SPECT image should tend to have similar grey level values. This regularization term is edge-preserving since it allows to apply a smoothness constraint, while preserving (anatomical) discontinuities. Besides, this *fuzzy* modeling, where each voxel can belong to several classes simultaneously, allows to take also into account the partial volume effect (the boundary between two or three structures of interest can fall in the middle of a voxel). Consequently, this strategy can be particularly well suited in order to recover small structures.

Furthermore, the introduction of the regularization term  $J_4$  does not affect the convexity of the NAS-RIF cost function, and therefore a unique solution to the problem is still guaranteed. A gradient-based iterative restoration algorithm or its conjugate version can be efficiently applied to minimize this new convex cost function (Eq. (3)). In addition, since the proposed criterion is quadratic, many other optimization methods can be used.

### 3. GENERATION OF THE 3D MRI ATLAS

The database of MRI volumes used for building a probabilistic atlas of human neuro-anatomy were acquired as part of the ICBM project [3]. This database contains 152 young, normal subjects (86 males; 66 females; age  $23.4 \pm 4.1$ ), and was scanned on a Philips Gyroscan ACS 1.5 Tesla system at the Montreal Neurological Institute using a T1-weighted 3D spoiled gradient echo acquisition with sagittal volume excitation (TR= 18, TE= 10, flip angle =  $30^\circ$ , 140 – 180 sagittal slices).

When image volumes are transformed into a common stereotaxic space and re-sampled on the same voxel grid such that all brains have the same orientation and size, voxel-by-voxel comparisons across data volumes from different populations are possible, since each voxel  $(i, j, k)$  corresponds to the same  $(x, y, z)$  point in the brain-based coordinate system.

After preprocessing to correct for intensity non-uniformity, the data are linearly registered into stereotaxic space and re-sampled onto a 1mm isotropic grid. The resulting volume is automatically classified into GM, WM, and CSF components and the cortical surface is automatically extracted. The statistical probability anatomy map is created with voxel-by-voxel averaging of label volumes from tissue classified data from subjects to yield spatial priors that can be used in classification procedures. At each voxel, the probability is proportional to the number of voxels associated to label, divided by the total number of subjects (i.e., the empirical proportion). (see Fig. 2).

### 4. 3D/3D REGISTRATION

The 3D registration method used in our application is based on mutual information (MI) and is fully described in [13]. The MI registration criterion  $C(\theta)$  between the input MRI and SPECT volumes describes the amount of information in the joint histogram of the images; hence its maximization results in the best match of intensity correspondences between the images for registration. The optimal set of registration parameters  $\theta_{\text{optimal}}$  is then found by maximizing  $C(\theta)$ , where the vector  $\theta$  is simply estimated by the Powell's method [14]. The images are smoothed slightly in order to make the cost function  $C(\theta)$  as smooth as possible to give faster convergence and less chance of finding bad local minima (related to a wrong registration). The code used to register the MRI image to the SPECT image is mainly inspired from the software package Statistical Parametric Mapping (SPM)<sup>1</sup>.

### 5. EXPERIMENTAL RESULTS

Restoration simulations were performed on thirty SPECT images of different epileptic patients. The SPECT data set were acquired with a triple-head  $\gamma$ -camera (Picker Prism, Marconi Irix, Cleveland, OH) equipped with low-energy, high-resolution parallel-holes collimators. 90 projections of 50 seconds each were obtained on  $128 \times 128 \times N$  voxels with 1.85 mm isotropic voxels and  $N \in [69, 103]$ .

The initial inverse FIR filter required by the NAS-RIF algorithm is the Kronecker delta function [15] and the size of this inverse filter is  $3 \times 3 \times 3$  pixels. Besides, we have used  $\gamma = 0$  because the background of SPECT images is not completely black.

Figure 2 presents an axial cross-section of the MRI atlas with the three statistical probability maps. Figure 3 shows examples of brain SPECT image deconvolution obtained by our 3-D blind deconvolution approach.

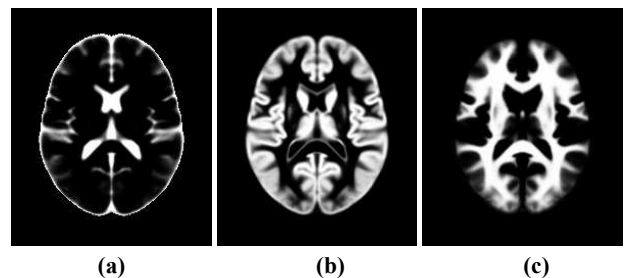


**Fig. 2.** Cross-section of the MRI atlas showing the three statistical probability maps. (a) CSF, (b) Gray matter, (c) White matter.

The MRI atlas and SPECT images are initially positioned such that their centers coincide and that the corresponding scan axes of both images are aligned and have the same orientation. We have used the registration algorithm implemented in the software package (SPM)<sup>1</sup> to register the MRI atlas to the SPECT image. During the registration procedure, the grid points of the MRI atlas will not necessarily coincide with the grid points of the SPECT image. Therefore, we used cubic-spline interpolation.

<sup>1</sup>The software package SPM can be downloaded at <http://www.fil.ion.ucl.ac.uk/spm/>

The proposed method allows to increase the resolution and contrast of the SPECT images without amplifying too much the mottle into the different pre-detected anatomical regions.

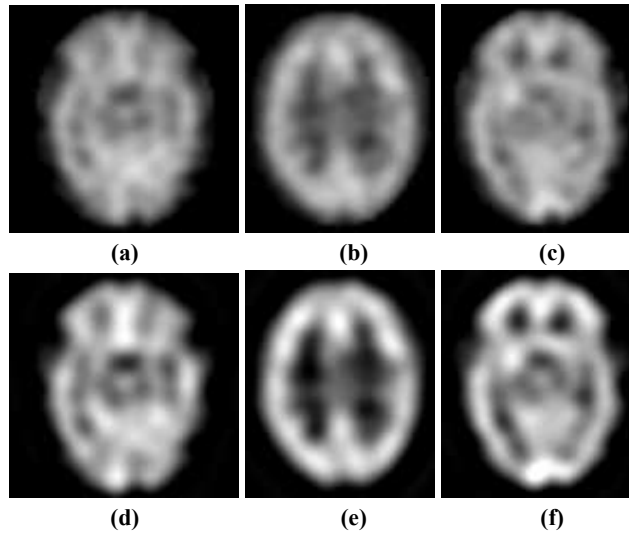


**Fig. 3.** Restoration results. (a) (b) (c) SPECT original cross-sections. (d) (e) (f) corresponding restored images.

## 6. CONCLUSION

In this paper, we have presented a fully automated 3D restoration method of brain functional SPECT images (after tomographic reconstruction). This method exploits a reliable (high resolution anatomical) MRI atlas via a new regularization term which efficiently stabilizes the inverse solution of the NAS-RIF restoration procedure. Besides, this regularization term is convex, (and thus does not affect the convexity of the original NAS-RIF cost function), edge-preserving, take into account the partial volume effect and can thus be particularly well suited to recover small structures in a SPECT image. Finally, contrary to other multi-modal restoration techniques, it does not require an additional MRI scan of the patient. This method has been tested on a number of SPECT images, demonstrating its efficiency and robustness. This 3D blind restoration technique is completely data driven, and could be implemented to automatically process massive numbers of 3D SPECT studies.

## 7. REFERENCES

- [1] D. Kundur and D. Hatzinakos, "Blind image deconvolution," *IEEE Signal Processing Magazine*, vol. 13, no. 3, pp. 43–64, 1996.
- [2] S. Benamer, M. Mignotte, J. Meunier, and J-P Soucy, "An edge-preserving anatomical-based regularization term for the NAS-RIF restoration of SPECT image," in *13th IEEE International Conference on Image Processing*, Atlanta, GA, USA, October 2006, pp. 1177–1180.
- [3] J.C. Mazziotta, A.W. Toga, A. Evans, P. Fox, and J. Lancaster, "A probabilistic atlas of the human brain : Theory and rationale for its development. the international consortium for brain mapping (ICBM)," *NeuroImage*, vol. 2, no. 1, pp. 89–101, 1995.
- [4] K. Van Leemput, F. Maes, D. Vandermeulen, and P. Suetens, "Automated model-based tissue classification of MR images of the brain," *IEEE Transactions on Medical Imaging*, vol. 18, no. 10, pp. 897–908, 1999.
- [5] K. Van Leemput, F. Maes, D. Vandermeulen, A. Colchester, and P. Suetens, "Automated segmentation of multiple sclerosis lesions by model outlier detection," *IEEE Transactions on Medical Imaging*, vol. 20, no. 8, pp. 677–688, 2001.
- [6] M. Lorenzo-Valdes, G. Sanchez-Ortiz, A. Elkington, R. Mohiaddin, and D. Rueckert, "Segmentation of 4D cardiac MR images using a probabilistic atlas and the EM algorithm," *Medical Image Analysis*, vol. 8, no. 3, pp. 255–265, 2004.
- [7] H.J. Park, C.-F. Westin, M. Kubicki, S. Maier, M. Niznikiewicz, A. Baer, M. Frumin, R. Kikinis, F. Jolesz, R. McCarley, and M. Shenton, "White matter hemisphere asymmetries in healthy subjects and in schizophrenia : a diffusion tensor MRI study," *NeuroImage*, vol. 23, no. 1, pp. 213–223, 2004.
- [8] I. Sluimer, M. Prokop, and B. van Ginneken, "Toward automated segmentation of the pathological lung in CT," *IEEE Transactions on Medical Imaging*, vol. 24, no. 8, pp. 1025–1038, 2005.
- [9] H. Park, P. Bland, and C. Meyer, "Construction of an abdominal probabilistic atlas and its application in segmentation," *IEEE Transactions on Medical Imaging*, vol. 22, no. 4, pp. 483–492, 2003.
- [10] M. Chen, T. Kanade, D. Pomerleau, and H. Rowley, "Anomaly detection through registration," *Pattern Recognition*, vol. 32, no. 1, pp. 113–128, 1999.
- [11] M. Mignotte and J. Meunier, "Three-dimensional blind deconvolution of spect images," *IEEE Transactions on Biomedical Engineering*, vol. 4, no. 2, pp. 274–281, 2000.
- [12] D. Kundur and D. Hatzinakos, "A novel blind deconvolution scheme for image restoration using recursive filtering," *IEEE Transactions on Signal Processing*, vol. 46, no. 2, pp. 375–390, 1998.
- [13] W.M. Wells, P. Viola, H. Atsumi, S. Nakajima, and R. Kikinis, "Multi-modal volume registration by maximization of mutual information," *Medical Image Analysis*, vol. 1, no. 1, pp. 35–51, 1996.
- [14] M.J.D. Powell, "An efficient method for finding the minimum of a function of several variables without calculating derivatives," *Computer Journal*, , no. 7, pp. 152–162, 1964.
- [15] D. Kundur and D. Hatzinakos, "Blind image restoration via recursive filtering using deterministic constraints," in *Proc. International Conference on Acoustics, Speech, and Signal Processing*, 1996, vol. 4, pp. 547–549.